Tracing microplastic sources in urban water bodies combining their diversity, fragmentation and stability

Check for updates

Jinqiong Niu[1,2], Dongyu Xu[1,2], Wenqiang Wu[1,2] & Bo Gao [1,2] ✉

Tracing the sources of microplastics (MPs) across various environmental media is currently facing significant challenges due to their complex transportable features. In this study, we conducted a comprehensive identification of MP sources in Beijing water bodies by combining MP diversity and the conditional fragmentation model, thoroughly considering local multiple sources. The resemblance in MP community compositions implied shared or similar sources in rivers and lakes, and the sources were assorted and equivalent based on the high diversity of MPs. The conditional fragmentation model can act as a proxy of fragmentation characteristics of MPs. According to the model, suburban sewage, soils, and dry and wet deposition constituted significant sources of MPs in the rivers and lakes of Beijing. The extremely high abundance of MPs (520,000 items·m^{-3}) in suburban sewage also confirmed it as a potential source. For MPs with different polymer types and morphologies, non-fibrous polypropylene (PP) was primarily controlled by soils, whereas the contribution of sewage sludge to fibrous polyethylene terephthalate (PET) was notable. Our study provides insights for more accurate source apportionment and contributes to a better understanding of MP fate in urban environment.

As essential materials for society, global plastic production totaled 400.3 million tonnes (Mt) in 2022, representing a marginal growth compared to 394 Mt in 2021[1]. Plastic waste is constantly disintegrating into small particles, and one size fraction of particles smaller than 5 mm is called microplastics (MPs)[2]. Since the first report half a century ago[3], the occurrences of MPs have detected in various environmental compartments, including marine[4], freshwater[5], soil[6], and atmosphere[7]. The universal distribution of MPs has garnered growing concerns regarding their fate in the environment. Identifying the sources of MPs is crucial for understanding their environmental fate and implementing effective management strategies.

The source analysis of MPs is currently in an initial stage. Previous studies have primarily speculated potential sources of MPs based on their characteristics, such as chemical composition, colors, and shapes. For example, films and fibers may originate from consumer uses and clothing, respectively[8]. Common polymers in the environment, including polyethylene (PE), polypropylene (PP), and polystyrene (PS), are usually derived from packaging[9]. These experience-dependent methods possess a certain degree of subjectivity, whereas data-driven methods offer a solution to

overcome these limitations[10]. Wang et al. and Li et al. calculated the diversity index of MPs, which are comprehensive evaluation of richness and evenness, to reflect sources of MPs[11,12]. The conditional fragmentation model was proposed for use in source identification of MPs in soils by Wang et al.[13]. Zhang et al. established a source analysis model based on the aging characteristics of MPs[14]. However, the current studies still exhibit their constraints. First, the pollution sources they considered were not exhaustive, such as atmospheric and wet deposition. Second, their data were collected from the literature and lacked the detection of MPs in local environmental compartments. Therefore, the comprehensive source analysis of MPs based on field investigations is imperative.

Higher levels of urbanization bring about greater MP pollution[15,16]. Previous studies have reported that the abundance of MPs in surface water was negatively correlated with the distance to the city[17,18]. The MPs in urban water bodies exhibit not only high abundance but also complex and diverse sources due to high population density and anthropogenic disturbances. Significant quantities of MPs have been observed in municipal environmental management systems in every stage, such as wastewater treatment

[1]State Key Laboratory of Simulation and Regulation of Water Cycle in River Basin, China Institute of Water Resources and Hydropower Research, 100038 Beijing, China. [2]Department of Water Ecology and Environment, China Institute of Water Resources and Hydropower Research, 100038 Beijing, China. ✉e-mail: gaobo@iwhr.com

Fig. 1 | Study area and sampling sites for MPs in Beijing. The sampling action carried out in 2021 across three water bodies in Beijing, including rivers (R1–R13), lakes (L1–L5) and suburban sewage (S1–S14). Sampling sites of rivers (gray dot), lakes (blue dot) and suburban sewage (red dot) are marked on the map.
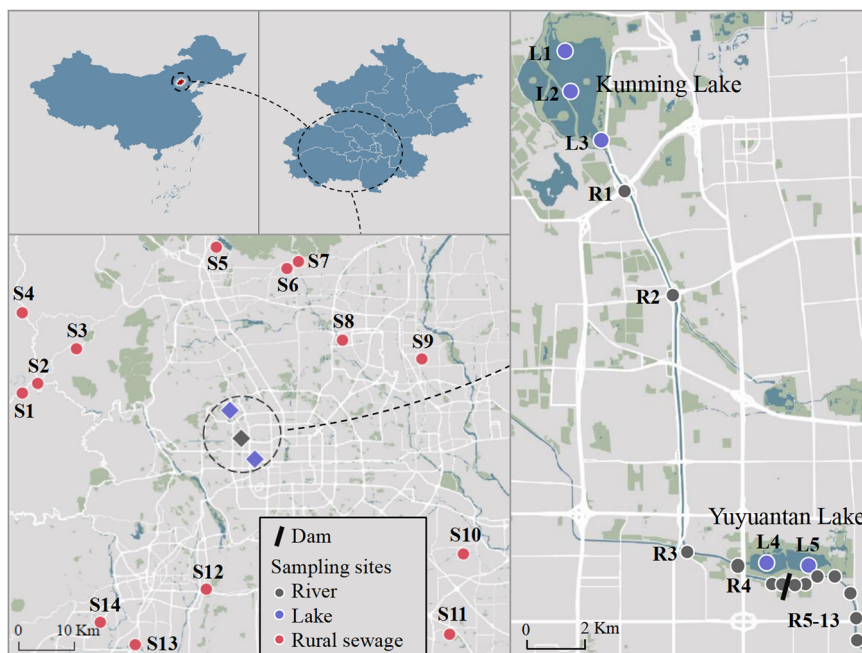
plants (WWTPs) and sewage sludge treatment facilities[19,20]. Soil, precipitation and atmosphere also contribute to MP pollution in urban environments[6,21]. Meanwhile, suburban areas encompass various industries, including agriculture and manufacturing, which are commonly accompanied by the discharge of sewage containing abundant untreated MPs. However, there is a scarcity of research regarding the sources of MPs in urban environments at present, and a comprehensive consideration of these sources is notably absent. Thus, a holistic comprehension of MP sources in different urban water bodies is essential to understand the transport and fate of MPs in ecosystems.

Therefore, our study focused on MP contamination in typical water bodies in China's capital, Beijing, including rivers, lakes and suburban sewage (Fig. 1). The objectives of this study were to: 1) determine the occurrence characteristics and assess the pollution risk of MPs in different water bodies; 2) analyze the potential sources of MPs in water bodies based on the spatial differentiation and diversity of the MP community; and 3) identify the sources of MPs using the conditional fragmentation model.

Results

Abundance of MPs
MPs were found at all the sampling sites in this study, with a total of 2306 particles observed across the 39 field samples. The abundances of MPs in different water bodies were summarized in Supplementary Table 1. The average abundance of MPs in rivers before precipitation was 2421 ± 2379 items·m^{-3}, ranging from 105 to 8000 items·m^{-3}. After precipitation, the average abundance of MPs in rivers increased to $16,590 \pm 6312$ items·m^{-3} in the range of 8267 to 27,867 items·m^{-3}. Moreover, the MP abundance in the sample from the rain event was 296,000 items·m^{-3}. The abundance of MPs in lakes ranged from 1789 to 7895 items·m^{-3}, and the mean MP abundance was 4758 ± 2294 items·m^{-3}. The MP abundance in the suburban sewage varied among sampling sites and ranged from 160,000 to 896,000 items·m^{-3}, with an average of $520,000 \pm 241,859$ items·m^{-3}.

Polymer compositions of MPs
A total of nine polymer types of MPs were identified: PE, PP, PS, polyethylene terephthalate (PET), nylon (PA), ethylene vinyl acetate (EVA), polymethyl methacrylate (PMMA), polyvinyl chloride (PVC), and polytetrafluoroethylene (PTFE). The proportions of the polymers in rivers before precipitation were as follows: PP (37.5%) >PS (24.1%) >PE (17.4%) >PA (13%) >PET (8%). After precipitation, the river samples were composed mainly of PE (61%) and PP (29%) with some EVA, PET, PS, PA, and PTFE, which was consistent with the sample from the rain event except for PET. The proportions of the polymers in lakes were as follows: PE (41.2%) >PS (28.3%) >PP (20.8%) >PET (5.3%) >PA (4.4%). Suburban sewage samples contained mostly PE (64.6%) and PP (30.8%) with small amounts of PS, EVA, PET, PMMA, PA, and PVC.

Morphotypes of MPs
The morphotypes of MPs in this study were classified into fragment, fiber, and film. Fragments were dominant at all sites and contributed to 88.3% of the total MPs, followed by films (5.9%) and fibers (5.8%). The percentage contribution of MPs with different morphologies varied across water bodies: fragments, 71.7–91.5%; films, 2.3–22.6%; and fibers, 5.7–8%.

Size distribution of MPs
The particle size of all detected MPs in this study ranged from 10 to 5000 µm. The MP sizes were classified into four classes: 10–100 µm, 100–300 µm, 300–1000 µm, and 1000–5000 µm, of which MPs with sizes <300 µm were defined as small-sized microplastics (SMPs) and >300 µm MPs were defined as normal-sized microplastics (NMPs).

The SMPs accounted for 94.3% of the total MPs in water bodies. The mean size of MPs in rivers before precipitation was 172.24 ± 303.34 µm, and the 100–300 µm MPs (46.2%) showed the highest proportion. After precipitation, 10–100 µm MPs (61.7%) were dominant in rivers, and the mean size of MPs decreased to 130.14 ± 236.44 µm. The mean size of MPs in the rainwater sample was 108.33 ± 69.01 µm, and all items identified were SMPs. The 10–100 µm MPs were also the major size type in lakes and suburban sewage, accounting for 54% and 55.3%, respectively. For MPs with different morphologies, the mean size of the fibers (450.71 µm) was significantly larger than that of the films (118.31 µm) and fragments (116.34 µm) ($p < 0.05$). In terms of polymer types, the mean size of PET (587.18 µm) was significantly larger than that of the other polymers (42.8–139.43 µm) ($p < 0.05$). Fibers and PET made up only a small part of SMPs (3.7% and 1.4%) but were the main component of NMPs (41.2% and 34.4%) (Fig. 2a).

Pollution risk of MPs
The MP pollution risks in different water bodies were calculated (Supplementary Table 3). The *PLI*, *H* and *PRI* in rivers were 0.2, 5.36 and 6.43, respectively. The *PLI* of Kunming Lake was 0.43 (unpolluted), and the *PLI* of

Yuyuantan Lake was 1.06 (level I). The *H and PRI* for lakes were 12.89 (level II) and 7.99 (level I), respectively. The *PLI* and *H* of suburban sewage were

68.11 (level IV) and 13.02 (level II), respectively. The overall pollution risk of MPs in suburban sewage was calculated as level IV, and the *PRI* values revealed medium (level II) to very high (level V) risks among sampling points.
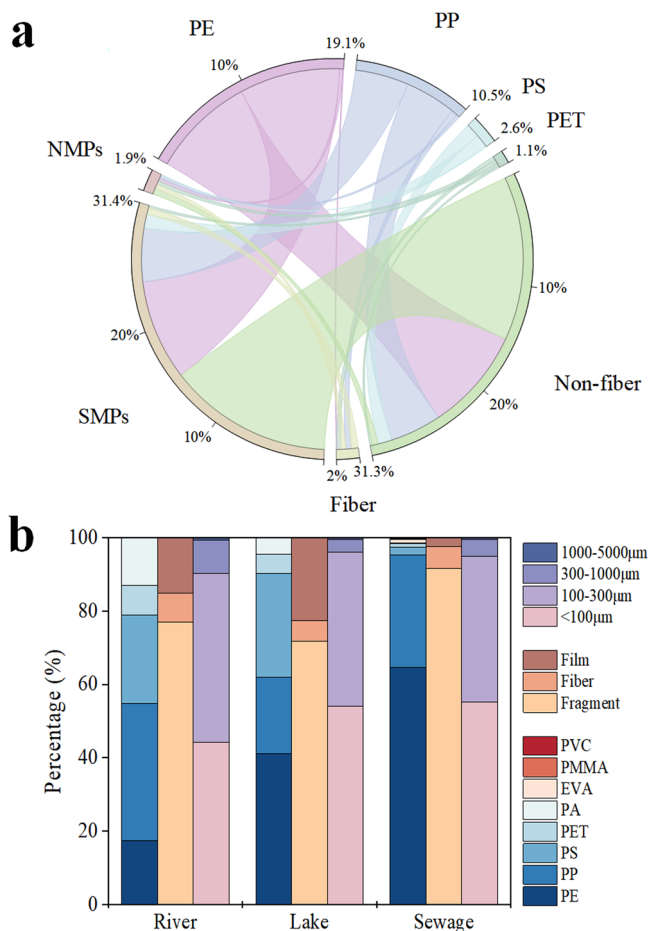
Fig. 2 | Distribution of polymer types, morphotypes, and sizes for MPs in Beijing. **a** Chord diagram of MPs shape and size types of different polymer types. **b** The proportion of polymer types (PE, PP, PS, PET, PA, EVA, PMMA and PVC), morphotypes (fragment, fiber and film), and sizes (<100, 100–300, 300−1000 and 1000–5000 μm) in different water bodies in Beijing.

Discussion

Occurrence and pollution risk of MPs in different water bodies

MPs were found in all samples, which indicated the ubiquity of MPs in typical water bodies in Beijing (Supplementary Fig. 1). The MP abundance in lakes exceeded that in rivers, and an extremely high abundance of MPs was detected in suburban sewage. In rivers, the average abundance of MPs was 2421 ± 2379 items·m^{-3}, and the MPs had spatial heterogeneity (Supplementary Table 1). Many factors can influence the organization of MPs, including source input, MP properties, weather conditions and water area features[22,23]. The spatial distribution of MPs in rivers in this study was mainly affected by dams. The highest abundance of MPs was detected in front of the dam (R6), while it greatly decreased after the dam. This suggested the interception of MPs by the dam. The river confluence (R3) was also an hotspot of MPs, attributed to the vortex capturing effect generated by turbulence[24]. The mean abundance of MPs in lakes (4758 items·m^{-3}) was higher than that in rivers. The results revealed that lakes were potential sinks of MPs in urban water environments. The MP abundance in suburban sewage (520,000 items·m^{-3}) was two orders of magnitude higher than that in rivers and lakes, which indicated an important source of MPs. The abundance distribution of MPs in suburban sewage was nonuniform. The differences in land use patterns and population size may have contributed to the disparities in MPs we observed among sewage. Nevertheless, even the lowest abundance of MPs in sewage reached 160,000 items·m^{-3}. These results highlighted that suburban sewage could be an important source of MPs in urban water bodies.

Here, we have compared our results with previous reports from urban rivers, lakes and WWTP inlet water (Table 1)[25–46]. The MPs pollution in rivers in this study was moderate compared with that of other urban rivers, which was higher than that in earlier studies in Beijing[30,32]. The MPs abundance in lakes in Beijing was almost equivalent to that in previous surveys on MPs in urban lakes[17,33]. Compared with data reported from the influent in WWTP, the abundance of MPs (520,000 items·m^{-3}) in sewage in Beijing ranked third. Although the population density and urbanization level are related to the level of MP pollution[16], the comparison results in this study showed that the MP levels in suburban areas were no lower than those in most urban areas. This may be attributed to the differences in environmental protection measures between urban and suburban areas. Wastewater treatment facilities in suburban areas are often inadequate, and abundant wastewater and the MPs they

Table 1 | Average abundance of MPs in urban water bodies from different cities

Water body	City	Abundance (items·m^{-3})	Reference	Water body	City	Abundance (items·m^{-3})	Reference
River	Chongqing	105000	25	Wastewater	Denmark	7216000	35
	Shanghai	27840	26		Helsinki	567800	36
	Guangzhou	19860	18		**Beijing**	**520000 ± 241859**	**This study**
	Chengdu	15880	27		Charleston	146750	37
	Beijing	**2421 ± 2379**	**This study**		Mount Pleasant	133091	37
	Nanning	2345	28		Wuhan	79900	38
	Sichuan	1947	29		Changsha	62165	39
	Beijing-1	1772	30		Vancouver	31100	40
	Ningbo	1658	31		Zhengzhou	16000	41
	Beijing-2	1164	32		Hong Kong	10360	42
Lake	**Beijing**	**4758 ± 2294**	**This study**		Xiamen	6550	43
	Wuhan	4709	17		Italy	2500	44
	Yueyang	4664	33		Hangzhou	1193	45
	Changsha	4242	34		Wuxi	280	46

The bold values are data from this study.

Fig. 3 | Pollution risk degree of MPs in Beijing.
Colors represent polymeric risk indexes and circles
with different sizes represent pollution risk indexes.
Detailed information about the pollution risk of
MPs are given in Supplementary Table 3.
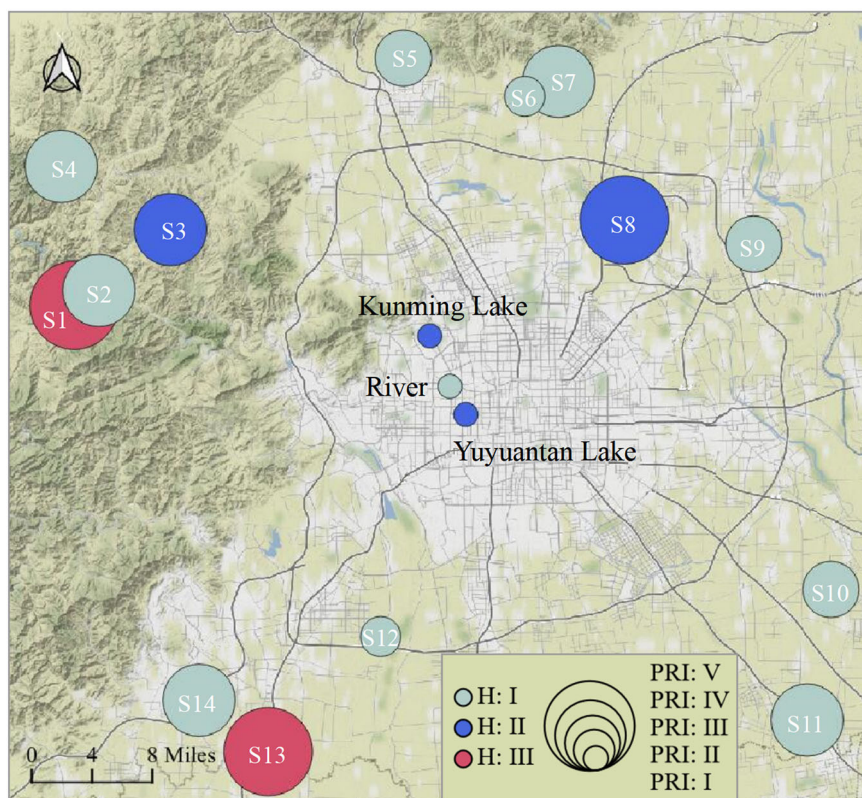
contain are discharged directly into the environment, which enhances the accumulation of MPs in suburban sewage.

In addition, wet deposition was an important factor affecting the MP loads in the study region. In rivers, the abundance of MPs after rain (16,590 items·m^{-3}) was one order of magnitude higher than that before rain (2421 items·m^{-3}). Many studies found higher MP abundance after precipitation[5,47]. This may be due to three reasons, including direct input of MPs in rainwater, stronger erosion of surface runoff, and resuspension of MPs in sediment[48,49]. In this study, a high abundance of MPs (296,000 items·m^{-3}) was detected in the sample from the rainfall event, which was in accord with our previous study[21]. The input of MPs in the rainwater could be the reason for the increased MP abundances post-rainfall in the study area. These results indicated that rainfall was a considerable source of MP diffuse pollution.

In this study, the *PLI*, *H*, and *PRI* of rivers, lakes and suburban sewage in Beijing were evaluated (Fig. 3). The *PLI* values would increase with the rise of MPs abundances. The *PLI* indicated that the MPs pollution load in most sampling sites of rivers and lakes was negligible (*PLI* < 1). The rivers after precipitation were polluted with MPs (*PLI* > 1), but the pollution load was still at a low level. The *PLI* level of all sampling points in suburban sewage reached the highest grade (level IV) except S12, which showed that suburban sewage had a high pollution load of MPs.

The *H* in different water bodies in Beijing was evaluated taking the chemical toxicity coefficient into consideration. The categories of *H* are listed in Supplementary Table 2. The *H* values were found to differ among water bodies. The *H* of rivers (level I) and lakes (level II) was mainly determined by the proportion of PA and PS. The polymer risk was higher at the sampling sites with a high proportion of PA or PS. For suburban sewage, the polymeric risks varied from level I to III. The sampling sites in suburban sewage had high chemical risk index due to the presence of PVC and PMMA with high hazard scores.

The *PRI* was employed by combining *PLI* and *H* to evaluate the risk of MP pollution in diverse water bodies in Beijing. Based on the evaluation criteria (Supplementary Table 2), all *PRI* values in lakes and rivers were less than 150, indicating that the potential pollution risk of MPs was relatively low in clear water. The potential pollution risks of MPs depend on the

toxicity of MP polymers, as well as the pollution loads of MPs. The sampling site with the highest pollution load (*PLI* value) of MPs did not show the highest pollution risks (*PRI* value) consistently in this study. However, the two indices reflected similar trends. Both of them showed that the suburban sewage in Beijing had high pollution risks of MPs.

Spatial differentiations of MP community composition
Different water bodies harbored distinct MP community compositions, which facilitated the speculation of their potential sources. A comparison with MP features in rivers, lakes, and suburban sewage is presented in Fig. 2b. The distributions of MPs in rivers and lakes were mostly similar. The resembling community compositions of MPs were detected in rivers and lakes, and the predominant types included fragmented PE, PP, and PS. They are commonly used in packaging, construction, and electronics in everyday life[1]. The presence of shared or similar pollution sources could lead to analogous MP compositions. The rivers and lakes in this study both originate from Miyun Reservoir. It could be speculated that the source of MPs in rivers and lakes was relatively consistent. The characteristics of MPs varied greatly in sewage and clear water. The polymer types in sewage were more abundant, and PMMA and PVC were detected only in sewage. Fragments and SMPs also predominated in the suburban sewage. This result was incompatible with some studies on the characteristics of MPs in wastewater. Previous studies reported the dominance of fibers in the influent of WWTPs due to the high impact of washing activities on MP release[50]. This difference indicated that there were other major sources of MPs in suburban sewage in addition to domestic wastewater, such as agriculture[51].

Moreover, we used PCoA to visualize whether polymer types within the same water body were closer to each other than samples from different water bodies and to further present the differences between water bodies (Fig. 4a). Rivers and lakes overlapped the most based on the similarity of polymer types. Suburban sewage samples were separated from rivers and lakes. Stacked bar charts with the proportion of each polymer type within each water body help visualize what polymer types may be driving patterns (Fig. 2b). The samples from suburban sewage were unique to rivers and lakes, which may be due to the higher proportion of PE and lower occurrence of PS in sewage.
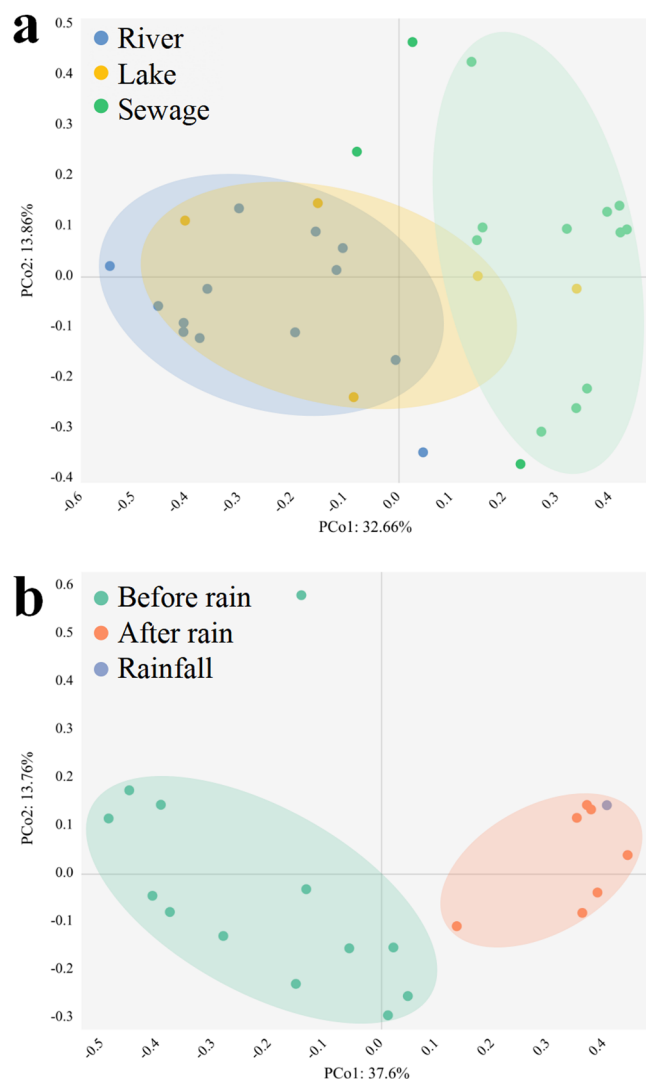
Fig. 4 | Principal coordinates analysis (PCoA) plots of polymer types. The polymer types of MPs **a** in different water bodies and **b** in the rivers (before and after rain) and rainfall based on PCoA analysis using the weighted Bray−Curtis metric are displayed on the figure.

Rainfall not only led to an increase in MP abundance but also reorganized the MPs in rivers (Supplementary Fig. 2). The chemical composition became richer after rain. And due to the high proportion of PE (63.5%) in the input rainwater, the main polymer type shifted from PP to PE in rivers after precipitation. Fragments and SMPs also dominated the MPs after rain, and their proportions increased. This implied that the increased PE after rainfall was mainly composed of small fragments. The PCoA showed a complete separation between polymer types before and after rain (Fig. 4b). The separation seems to be driven by the large proportion of PE after rain. The rainfall samples overlapped with river samples after rain, further suggesting precipitation as a source of MPs to surface waters.

Diversity as an indicator of MP sources

The Simpson index (D) and the Shannon index (H') were adopted as quantitative measures to assess the diversity of MPs (Supplementary Fig. 3). They could serve as synthetic indicators to characterize the traits and indicate the sources of MPs in various water bodies[12]. The MPs in rivers and lakes represented low abundance with high diversity. In contrast, suburban sewage indicated high MP abundance and low MP diversity. The *MDII* and *MHII* in rivers and lakes were similar and both higher than those in suburban sewage. The polymer types and shapes were major contributors to the

difference in MP diversity between clean water and sewage. Although the overall number of polymer types identified in sewage was higher, the diversity was lower, which was due to the inhomogeneous distribution of the polymers. In most cases, the richness of polymers in a single suburban sewage sample was less than that in rivers and lakes. These results implied that the sources of MPs in rivers and lakes were multiple and contributed equivalently, while one or a limited number of MP sources made a dominant contribution to suburban sewage. Agriculture was the main economic activity in suburban areas in this study. The extensive application of plastic equipment and materials in agricultural practices, such as greenhouses and soil mulch, constitutes a significant source of MPs in suburban sewage.

Precipitation could also influence MP diversity in surface water. The diversity of polymer types, shapes and sizes of MPs all decreased after rain in this study. This occurred due to the transition from a diverse contribution of MPs from various sources to a dominant contribution from rainfall. However, previous study has shown that rainfall leads to an increase in MP diversity[32]. This discrepancy between the previous study and our results may be attributed to the difference in the sampling period. Although precipitation enriched the MP sources, the characteristics of MPs in the early period after rain were consistent with those in rainfall, and the diversity was relatively low.

MP source identification based on the conditional fragmentation model

We used the conditional fragmentation model to depict the fragmentation and stability in typical water bodies in Beijing (Fig. 5a). The range parameter λ value was associated with the particle size of MPs. The percentage of SMPs in lakes reached 96.02%, and the λ value in lakes was obviously larger than that in other water bodies. The λ values in this study surpassed those found in containers, rubber, sewage sludge, and soils (Fig. 5d), highlighting the predominance of SMPs in urban water ecosystems. When the cumulative percentage reached 63.2%, the characteristic particle size of the MPs was 167, 109, 114, 117, and 109 μm in different water bodies, respectively. The values of α in all water bodies were greater than 1, indicating that larger MPs were more prone to weathering and fragmentation[13]. This suggested that MPs larger than the characteristic particle size still exhibited a tendency to undergo downsizing in this study. The order of α values in different water bodies was the same as that of λ values, which indicated that MPs in lakes have the highest stability. This was likely due to the impact of low disturbance on MPs in lakes compared to rivers and suburban sewage.

The size distribution of MPs was related to their morphologies and polymer types. This meant that the stability and fragmentation characteristics of MPs varied with different morphologies and polymer types. The characteristic particle sizes of non-fibrous MPs (fragment and film) and fibers were 110 and 413 μm, respectively. The λ and α values of non-fibrous MPs were both greater than those of fibers, which suggested that non-fibrous MPs have higher stability (Fig. 5b). This should be due to fiber with a higher surface area-to-volume ratio that was more susceptible to natural weathering[13]. For different polymer types, the stability of PET was significantly lower than that of other polymers (Fig. 5c). This was because fiber was the main morphotype of PET (68%), while the proportion of non-fibrous MPs in PS, PE and PP reached 96%.

The conditional fragmentation model can also be applied to the source identification of MPs[13]. The main sources of MPs, including atmospheric and wet deposition, soil, traffic, and wastewater/sludge, are presented by the parameter λ and α values in Fig. 5 and Supplementary Table 4. The λ and α values of all water bodies were in the range of those from atmospheric and wet deposition (Fig. 5d). This result indicated that atmospheric transport was an important source of MPs in the study area. And the effects of MP pollution from precipitation were persistent, not just in the period after rain. The λ and α values in rivers, sewage, and rainfall were close to those from soil samples, indicating that soil in cities may be a source for MPs in urban water bodies. Furthermore, the similarity of λ and α values between sewage and other water bodies (Supplementary Fig. 4), along with the high abundance of MPs in sewage, revealed that suburban sewage was also a contributor to MPs

Fig. 5 | Cumulative percentage and related modeling parameters of MPs in Beijing. The **a** water body, **b** morphotype, and **c** polymer type dependent size distribution of MPs following the conditional fragmentation law are displayed on the figure. The values from modeling parameters of different **d** water bodies, **e** morphotypes, and **f** polymer types are showed. The references are provided in Supplementary Table 4.
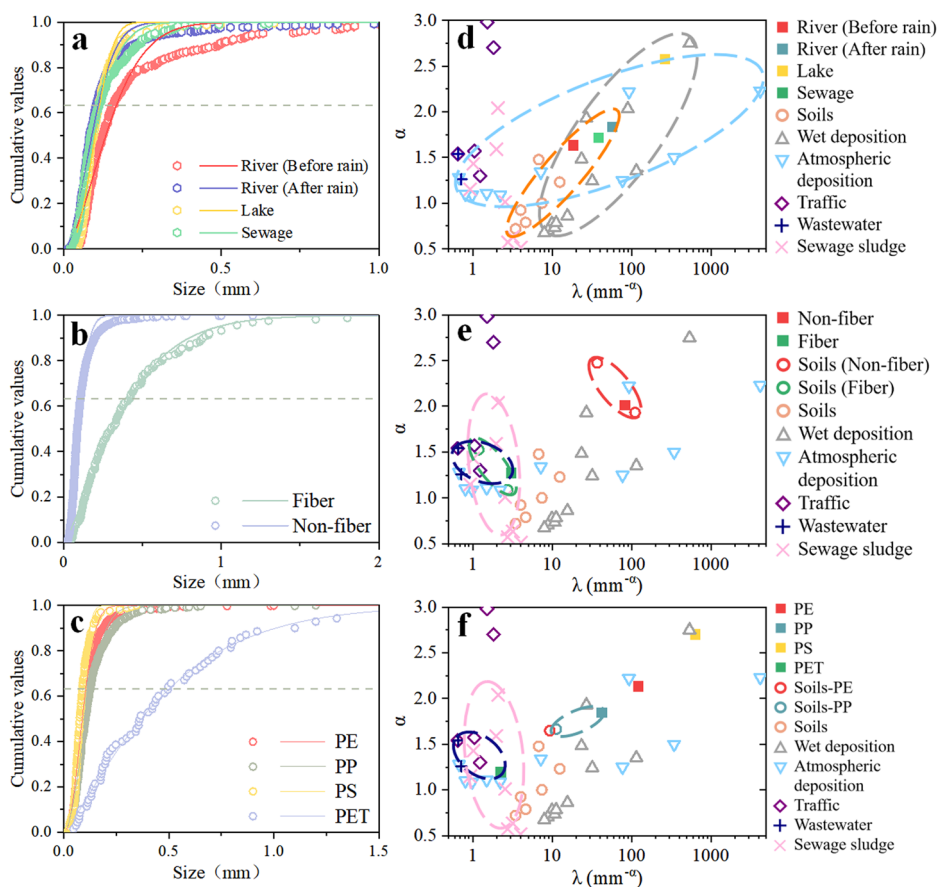
in urban water systems. The λ and α values of MPs in Beijing water bodies closely resembled those in suburban sewage but exhibited variations with wastewater from other regions, which underscored the importance of local field investigation in tracing the origins of MPs. While the data for atmospheric deposition also originated from other regions, they showed similarities with the λ and α values of MPs found in water bodies in Beijing, indicating the global transportable characteristics of MPs in the atmosphere.

For MPs with different morphologies, the parameter values of nonfibrous MPs and fibers were both similar to those observed in soils (Fig. 5e). For different polymer types, the parameter values obtained from PP also approximated soil samples (Fig. 5f). These results further indicated that soil was one of the sources of MPs in urban water systems. The λ and α values of PET and fiber were covered by the wastewater and sewage sludge groups (Fig. 5e, f). This was because fibrous PET is widely used in textiles such as clothing and bedding, and it is shed and discharged during washing[52]. The application of sewage sludge facilitated their entry into the environment. Additionally, the λ and α values of PET and fiber in this study were in proximity to those from urban roadside containers, suggesting that they are also influenced by traffic factors.

Environmental Implications
This study revealed the widespread presence of MPs in typical water bodies in Beijing, including rivers, lakes, and suburban sewage. The spatial differentiations of the MP community highlighted the variations in the MP sources across different water bodies. The conditional fragmentation model may help identify the local sources of MPs based on their fragmentation and stability. The results showed that diffuse pollution from dry and wet deposition and soils could be important sources of MPs in rivers and lakes where point pollution sources are well regulated. Of particular note is the high MP pollution risks posed by suburban sewage, which serves as a contributor to MP loads in urban water bodies. Prioritizing the management of MPs in suburban sewage should take precedence. Our study fills the research

gap in the fate and sources of MPs in urban water bodies and provides a basis for the effective pollution control of MPs. However, there is currently an absence of systematic approaches to characterize the contributions from these sources, which could be addressed in future study by exploring the application of fuzzy mathematics to quantify the sources of MPs.

Methods
Study area and sample collection
Beijing, the capital of China, is one of the first tier cities in the world, with a population of more than 21 million. Three representative water bodies in Beijing were selected to collect urban water samples, including rivers, lakes and suburban sewage. River samples were collected from the Jingmi diversion canal and the Yongding diversion channel. Lake samples were taken in Kunming Lake and Yuyuantan Lake. The sampling of sewage was performed in fiver suburbs of Beijing.

A total of 39 water samples were collected across different locations: thirteen from rivers (R1–R13), five from Lakes (L1–L5), and fourteen suburban sewage samples (S1–S14) (Supplementary Fig. 1). The annual precipitation in Beijing reached a record high of 627.4 mm in 2021, marking the highest level observed in the past two decades[21]. To understand the impact of precipitation, one rainwater sampling event was conducted on June 25, 2021. In addition, 7 river samples (R6-R12) were collected again after the rain. For rivers and lakes, the surface water samples collected in triplicate using a 10 L stainless-steel bucket and combined to form one composite sample (30 L). For suburban sewage and rain, 1 L water samples were collected using a stainless-steel bucket and automatic rainfall collector (APS−3A, China), respectively. All collected samples were transferred into brown glass bottles and taken to the laboratory for further analysis.

Laboratory analysis
The National Oceanic and Atmospheric Administration (NOAA) protocol was used to separate and extract MPs from collected samples[53]. In detail,

each water sample was filtered using a 5 mm stainless-steel sieve, and the filtrate was filtered through a metal filter membrane with an aperture of 10 μm by a vacuum pump (GM-0.33A, Jinteng, China). Then, the membrane was transferred into a 250 ml beaker and treated with 30% H_2O_2 for 24 h at 60 °C to decompose the organic matter. After completing digestion, the NaCl (6 g/20 ml) was added into the sample. The mixture was heated until dissolution of salt and transferred into a funnel for density separation. The supernatant was filtered through a 0.45 μm glass microfiber filter (Whatman GF/B) by vacuum filtration. Finally, the filter was stored in a Petri dish and dried at 50 °C for further analysis.

The samples were analyzed using a laser confocal microscope Raman spectrometer (DXR2xi, USA, 532 nm laser, Raman shift 50–3500 cm^{-1}) to identify the chemical composition of all the membrane particles. The polymer types were determined by matching the sample spectra with the spectrum in the instrument databases. Once the matching degree reached 70%, the particles were identified as MPs. The MP sizes were quantified through the measurement functionality of instrument, and the morphotypes were recorded based on their visual characteristics.

Quality assurance and quality control
Plastic materials were avoided in the entire process. The metal sieves and glassware were washed thoroughly before use via ultrasound, and all the experimental instruments were rinsed with ultrapure water at least three times. The MP analysis was conducted in a separate ultraclean laboratory, and the workplace was cleaned daily. Masks and cotton lab coats were worn during the experiment. The tools and samples were covered using aluminum foil or lids whenever possible. The field and laboratory blank test were assigned by 5 L of Milli-Q water (in triplicate), which were treated through the same procedure as that for the samples. MPs were not detected in the blank sample; thus, the contamination was considered to be negligible.

Diversity analysis
The Simpson index (D)[54] and the Shannon–Wiener index (H')[55] were calculated to represent the diversity of MPs in terms of polymer types, shapes, and size. The formulas to calculate $MDII$ and $MHII$ are as follows:

$$D = 1 - \sum_{i=1}^{S} \left(\frac{N_i - 1}{N - 1} \right)^2 \tag{1}$$

$$MDII = \sqrt[3]{D_{polymer} \times D_{shape} \times D_{size}} \tag{2}$$

$$H' = -\left(\sum_{i=1}^{S} \frac{N_i}{N} \times \ln\left(\frac{N_i}{N} \right) \right) \tag{3}$$

$$MHII = \sqrt[3]{H_{polymer} \times H_{shape} \times H_{size}} \tag{4}$$

where $D_{polymer}$, D_{shape}, and D_{size} are the Simpson index of polymer types, shapes and size of MPs, respectively. $H_{polymer}$, H_{shape}, and H_{size} are the Shannon–Wiener index of polymer types, shapes and size of MPs, respectively. N_i is the quantity of category i of MPs, S is the number of categories, and N is the total number of MPs. The Simpson integrated index of MPs ($MDII$) and the Shannon–Wiener integrated index of MPs ($MHII$) based on three indices reflected the comprehensive diversity of MPs.

Fragmentation and stability of MPs
We used the conditional fragmentation model to describe the fragmentation and stability of MPs[13]. This model can be defined as follows:

$$f(x) = 1 - e^{-\lambda x^\alpha} (x \geq 0) \tag{5}$$

$$x_0 = \lambda^{-1/\alpha} \tag{6}$$

where x is the size of the MPs, λ determines the range of MP sizes, and α depicts the fragmentation pattern. A higher value of λ indicates a higher degree of MP fragmentation, and a higher α value manifests a higher stability and a lower possibility of further fragmentation of MPs. According to the aging rate ($\lambda \alpha x^{\alpha-1}$), if $\alpha > 1$, the probability of MPs fragmentation would increase with larger MP sizes. Conversely, if $\alpha < 1$, smaller MPs will be more inclined to downsize further than larger MPs. x_0 is the characteristic particle size. When $x = x_0$, it can be defined as the size at which 63.2%, and the particles are smaller. Detailed derivation on the model is provided in the Supplementary Note 1.

Pollution risk assessments
The MPs pollution risk index (PRI) was calculated according to a previous study[56]. The pollution load index (PLI)[57] and the toxicity risks of polymers (H) of the MPs were used in the calculations. The PLI, H, and PRI were determined using the following formulas:

$$PLI_i = \frac{C_i}{C_0} \tag{7}$$

$$PLI_{zone} = \sqrt[n]{PLI_1 \times PLI_2 \times PLI_3 \times \cdots \times PLI_n} \tag{8}$$

$$H_i = \sum_{j=1}^{m} (P_{ji} \times S_j) \tag{9}$$

$$H_{zone} = \sqrt[n]{H_1 \times H_2 \times H_3 \times \cdots \times H_n} \tag{10}$$

$$PRI_i = H_i \times PLI_i \tag{11}$$

$$PRI_{zone} = \sqrt[n]{PRI_1 \times PRI_2 \times PRI_3 \times \cdots \times PRI_n} \tag{12}$$

where i represents a sampling site, n is the number of sampling sites in water bodies, C_i is the abundance of MPs at site i, and C_0 is the baseline abundance of MPs. We chose the predicted no effect concentration (6650 items·m^{-3}) as C_0 in this study[58]. j represents a polymer type, m is the number of identified polymer types, P_{ji} is the percentage of polymer j identified at site i, and S_j is the risk score for each detected polymer. The detected polymers and their score values were PE (11), PP (1), PET (4), PS (30), PA (47), EVA (9), PTFE (1), PMMA (1021), and PVC (10,001), respectively[59]. PLI_i, H_i, and PRI_i represent the indices calculated at site i, and PLI_{zone}, H_{zone}, and PRI_{zone} are the risks of the entire water body. The categories of PLI, H, and PRI are listed in Supplementary Table 2.

Data analysis
A one-way analysis of variance (ANOVA) was applied to determine significant differences using SPSS 19, and we assumed a significant difference when the p value < 0.05. The conditional fragmentation model was performed by SigmaPlot 14.0. The figures were created through ArcGIS 10.6 and Origin 2021. We used principal coordinate analysis (PCoA) to examine the polymer types in each water body, and the plots were run using Bray-Curtis distance.

Data availability
The data that support the findings of this study are available from the corresponding author upon reasonable request.

References
1. Plastics Europe. Plastics – the fast Facts 2023. https://plasticseurope.org/knowledge-hub/plastics-the-fast-facts-2023/ (2023).
2. Moore, C. J. Synthetic polymers in the marine environment: A rapidly increasing, long-term threat. *Environ. Res.* **108**, 131–139 (2008).

3. Carpenter, E. J. & Smith, K. L. Plastics on the Sargasso sea surface. *Science* **175**, 1240–1241 (1972).

4. Kanhai, L. D. K., Officer, R., Lyashevska, O., Thompson, R. C. & O'Connor, I. Microplastic abundance, distribution and composition along a latitudinal gradient in the Atlantic Ocean. *Mar. Pollut. Bull.* **115**, 307–314 (2017).

5. Xu, D., Gao, B., Wan, X., Peng, W. & Zhang, B. Influence of catastrophic flood on microplastics organization in surface water of the Three Gorges Reservoir. *China. Water Res.* **211**, 118018 (2022).

6. Zhang, M. et al. Small-sized microplastics (< 500 μm) in roadside soils of beijing, china: Accumulation, stability, and human exposure risk. *Environ. Pollut.* **304**, 119121 (2022).

7. Liu, K. et al. Source and potential risk assessment of suspended atmospheric microplastics in Shanghai. *Sci. Total Environ.* **675**, 462–471 (2019).

8. Helm, P. A. Improving microplastics source apportionment: a roleformicroplastic morphology andtaxonomy? *Anal. Methods* **9**, 1328–1331 (2017).

9. Hidalgo-Ruz, V., Gutow, L., Thompson, R. C. & Thiel, M. Microplastics in the marine environment: a review of the methods used for identification and quantification. *Environ. Sci. Technol.* **46**, 3060–3075 (2012).

10. Yao, Y., Luo, W. & Dai, Y. Research progress of data-driven methods in fault diagnosis of chemical process. *Chem. Ind. Eng. Prog.* **40**, 1755–1764 (2021).

11. Wang, T. et al. Preliminary study of the source apportionment and diversity of microplastics: Taking floating microplastics in the South China Sea as an example. *Environ. Pollut.* **245**, 965–974 (2019).

12. Li, C. et al. Microplastic communities" in different environments: Differences, links, and role of diversity index in source analysis. *Water Res.* **188**, 116574 (2021).

13. Wang, L. et al. Modeling the conditional fragmentation-induced microplastic distribution. *Environ. Sci. Technol.* **55**, 6012–6021 (2021).

14. Zhang, Z., Qin, X. & Zhang, Y. Using data-driven methods and aging information to quantitatively identify microplastic environmental sources and establish a comprehensive discrimination index. *Environ. Sci.Technol.* **57**, 11279–11288 (2023).

15. Dikareva, N. & Simon, K. S. Microplastic pollution in streams spanning an urbanisation gradient. *Environ. Pollut.* **250**, 292–299 (2019).

16. Huang, Y. et al. Coupled effects of urbanization level and dam on microplastics in surface waters in a coastal watershed of Southeast China. *Mar. Pollut. Bull.* **154**, 111089 (2020).

17. Wang, W., Ndungu, A. W., Li, Z. & Wang, J. Microplastics pollution in inland freshwaters of China: A case study in urban surface waters of Wuhan, China. *Sci. Total Environ.* **575**, 1369–1374 (2017).

18. Yan, M. et al. Microplastic abundance, distribution and composition in the Pearl River along Guangzhou city and Pearl River estuary, China. *Chemosphere* **217**, 879–886 (2019).

19. Alvim, C. B., Bes-Piá, M. A. & Mendoza-Roca, J. A. Separation and identification of microplastics from primary and secondary effluents and activated sludge from wastewater treatment plants. *Chem. Eng. J.* **402**, 126293 (2020).

20. Li, Q., Wu, J., Zhao, X., Gu, X. & Ji, R. Separation and identification of microplastics from soil and sewage sludge. *Environ. Pollut.* **254**, 113076 (2019).

21. Chen, Y. et al. Wet deposition of globally transportable microplastics (<25 μm) hovering over the megacity of Beijing. *Environ. Sci. Technol.* **57**, 11152–11162 (2023).

22. Wang, W., Yuan, W., Chen, Y. & Wang, J. Microplastics in surface waters of Dongting Lake and Hong Lake, China. *Sci. Total Environ.* **633**, 539–545 (2018).

23. Di, M. & Wang, J. Microplastics in surface waters and sediments of the Three Gorges Reservoir. *China. Sci. Total Environ.* **616-617**, 1620–1627 (2018).

24. Li, C. et al. Interventions of river network structures on urban aquatic microplastic footprint from a connectivity perspective. *Water Res.* **243**, 120418 (2023).

25. Fan, J., Zou, L. & Zhao, G. Microplastic abundance, distribution, and composition in the surface water and sediments of the Yangtze River along Chongqing City, China. *J. Soils Sediments* **21**, 1840–1851 (2021).

26. Zhang, J. et al. Microplastics in the surface water of small-scale estuaries in Shanghai. *Mar. Pollut. Bull.* **149**, 110569 (2019).

27. Li, X. et al. Microplastics in inland freshwater environments with different regional functions: A case study on the Chengdu Plain. *Sci. Total Environ.* **789**, 147938 (2021).

28. Zhang, X., Leng, Y., Liu, X., Huang, K. & Wang, J. Microplastics' pollution and risk assessment in an urban river: A case study in the Yongjiang River, Nanning City, South China. *Expo. Health* **12**, 141–151 (2020).

29. Zhou, G. et al. Distribution and characteristics of microplastics in urban waters of seven cities in the Tuojiang River basin. *China. Environ. Res.* **189**, 109893 (2020).

30. Zhang, B. et al. Comparative analysis of microplastic organization and pollution risk before and after thawing in an urban river in Beijing. *China. Sci. Total Environ.* **828**, 154268 (2022).

31. Xu, Y. et al. Microplastic pollution in Chinese urban rivers: The influence of urban factors. *Resour. Conserv. Recycl.* **173**, 105686 (2021).

32. Wei, Y., Dou, P., Xu, D., Zhang, Y. & Gao, B. Microplastic reorganization in urban river before and after rainfall. *Environ. Pollut.* **1**, 120326 (2022).

33. Wen, X. et al. Microplastics in surface water of a typical urban lake: A case study from Nanhu Lake, Yueyang City. *Environ. Chem.* **41**, 3579–3588 (2022).

34. Yin, L. et al. Microplastic pollution in surface water of urban lakes in Changsha, China. *Int. J. Environ. Res. Public. Health* **16**, 1650 (2019).

35. Simon, M., Alst, N. V. & Vollertsen, J. Quantification of microplastic mass and removal rates at wastewater treatment plants applying Focal Plane Array (FPA)-based Fourier Transform Infrared (FT-IR) imaging. *Water Res.* **142**, 1–9 (2018).

36. Talvitie, J., Mikola, A., Setälä, O., Heinonen, M. & Koistinen, A. How well is microlitter purified from wastewater? - A detailed study on the stepwise removal of microlitter in a tertiary level wastewater treatment plant. *Water Res.* **109**, 164–172 (2017).

37. Conley, K., Clum, A., Deepe, J., Lane, H. & Beckingham, B. Wastewater treatment plants as a source of microplastics to an urban estuary: Removal efficiencies and loading per capita over one year. *Water Res. X* **3**, 100030 (2019).

38. Liu, X., Yuan, W., Di, M., Li, Z. & Wang, J. Transfer and fate of microplastics during the conventional activated sludge process in one wastewater treatment plant of China. *Chem. Eng. J.* **362**, 176–182 (2019).

39. Long, Y. et al. Microplastics removal and characteristics of constructed wetlands WWTPs in rural area of Changsha, China: A different situation from urban WWTPs. *Sci. Total Environ.* **811**, 152352 (2022).

40. Gies, E. et al. Retention of microplastics in a major secondary wastewater treatment plant in Vancouver, Canada. *Mar. Pollut. Bull.* **133**, 553–561 (2018).

41. Ren, P., Dou, M., Wang, C., Li, G. & Jia, R. Abundance and removal characteristics of microplastics at a wastewater treatment plant in Zhengzhou. *Environ. Sci. Pollut. Res. Int.* **27**, 36295–36305 (2020).

42. Cao, Y. et al. Intra-day microplastic variations in wastewater: A case study of a sewage treatment plant in Hong Kong. *Mar. Pollut. Bull.* **160**, 111535 (2020).

43. Long, Z. et al. Microplastic abundance, characteristics, and removal in wastewater treatment plants in a coastal city of China. *Water Res.* **155**, 255–265 (2019).

44. Magni, S. et al. The fate of microplastics in an Italian Wastewater Treatment Plant. *Sci. Total Environ.* **652**, 602–610 (2019).
45. Wei, S. et al. Characteristics and removal of microplastics in rural domestic wastewater treatment facilities of China. *Sci. Total Environ.* **739**, 139935 (2020).
46. Lv, X. et al. Microplastics in a municipal wastewater treatment plant: Fate, dynamic distribution, removal efficiencies, and control strategies. *J. Clean. Prod.* **225**, 579–586 (2019).
47. Piñon-Colin, T. D. J., Rodriguez-Jimenez, R., Rogel-Hernandez, E., Alvarez-Andrade, A. & Wakida, F. T. Microplastics in stormwater runoff in a semiarid region, Tijuana, Mexico. *Sci. Total Environ.* **704**, 135411 (2020).
48. Xia, W., Rao, Q., Deng, X., Chen, J. & Xie, P. Rainfall is a significant environmental factor of microplastic pollution in inland waters. *Sci Total Environ.* **732**, 139065 (2020).
49. Barrows, A. P. W., Christiansen, K. S., Bode, E. T. & Hoellein, T. J. A watershed-scale, citizen science approach to quantifying microplastic concentration in a mixed landuse river. *Water Res.* **147**, 382–392 (2018).
50. Hamidian, A. H. et al. A review on the characteristics of microplastics in wastewater treatment plants: A source for toxic chemicals. *J. Clean. Prod.* **295**, 126480 (2021).
51. Kim, S.-K., Kim, J.-S., Lee, H. & Lee, H.-J. Abundance and characteristics of microplastics in soils with different agricultural practices: Importance of sources with internal origin and environmental fate. *J. Hazard. Mater.* **403**, 123997 (2021).
52. Browne, M. A. et al. Accumulation of microplastic on shorelines woldwide: sources and sinks. *Environ. Sci. Technol.* **45**, 9175–9179 (2011).
53. Masura, J. et al. *Laboratory Methods for the Analysis of Microplastics in the Marine Environment: recommendations for quantifying synthetic particles in waters and sediments*. NOAA Technical Memorandum, NOS-OR&R-48 (NMFS Scientific Publications Office, Seattle, 2015).
54. Simpson, E. H. The measurement of diversity. *Nature* **163**, 688 (1949).
55. Shannon, C. E. A mathematical theory of communication. *Bell Syst. Tech. J.* **27**, 623–656 (1948).
56. Kabir, A. et al. Assessing small-scale freshwater microplastics pollution, land-use, source-to-sink conduits, and pollution risks: perspectives from Japanese rivers polluted with microplastics. *Sci. Total Environ.* **768**, 144655 (2021).
57. Tomlinson, D. L., Wilson, J. G., Harris, C. R. & Jeffrey, D. W. Problems in the assessment of heavy metal levels in estuaries and the formation of a pollution index. *Helgol. Meeresunters.* **33**, 566–575 (1980).
58. Everaert, G. et al. Risk assessment of microplastics in the ocean: Modelling approach and first conclusions. *Environ. Pollut.* **242**, 1930–1938 (2018).
59. Lithner, D., Larsson, A. & Dave, G. Environmental and health hazard ranking and assessment of plastic polymers based on chemical composition. *Sci. Total Environ.* **409**, 3309–3324 (2011).

Author contributions
Jinqiong Niu: Investigation, Methodology, Writing - Original draft preparation. Bo Gao: Project administration, Data curation, Funding acquisition, Formal analysis, Writing - Reviewing and editing. Wenqiang Wu: Supervision, Formal analysis. Dongyu Xu: Methodology, Writing - Reviewing and editing.

Competing interests
The authors declare no competing interests.

Additional information
Supplementary information The online version contains supplementary material available at https://doi.org/10.1038/s41545-024-00329-2.

Correspondence and requests for materials should be addressed to Bo Gao.

Reprints and permissions information is available at http://www.nature.com/reprints

Publisher's note Springer Nature remains neutral with regard to jurisdictional claims in published maps and institutional affiliations.